PAPER

Check for updates

Photochemical formation of water-soluble oxyPAHs, naphthenic acids, and other hydrocarbon oxidation products from Cook Inlet, Alaska crude oil and diesel in simulated seawater spills†

Maxwell L. Harsha, [ID] *[a] Zachary C. Redman, [ID] [c] Josh Wesolowski,[c] David C. Podgorski [ID] [abc] and Patrick L. Tomco [ID] [ac]

Hydrocarbon oxidation products (HOPs) formed from crude oil and diesel were formed from laboratory simulated spills at four different periods (1, 4, 7, and 10 days) under environmental conditions that mimicked those in Cook Inlet, Alaska. Two sets of analyses were performed to identify and characterize the HOPs. The first set of analyses performed was non-targeted and included high-resolution mass spectrometry and fluorescence excitation-emission matrix spectroscopy. Liquid chromatography coupled with an Orbitrap mass spectrometer uncovered that HOPs formed from Cook Inlet (CI) crude oil and diesel are relatively reduced, saturated, and unsaturated compounds. The molecular compositions of HOPs from crude oil are more aromatic, whereas those formed from diesel are more aliphatic. Moreover, molecular signatures of naphthenic acids, a class of toxicants, in HOPs are reported. Six unique chemical features of HOPs were revealed by fluorescence excitation-emission matrix spectroscopy, including two unique petroleum signatures. The parallel factor model for fluorescence excitation-emission matrix spectroscopy accurately tracks temporal compositional changes of HOPs. The second set of analyses was targeted and included the quantification of polycyclic aromatic hydrocarbons (PAHs) and oxygenated polycyclic aromatic hydrocarbons (oxyPAHs) in HOPs using tandem mass spectrometry. Two oxyPAHs, phenanthrenequinone, and 1,4-anthraquinone were quantified in HOPs formed from CI crude oil and related to eleven PAHs. The results from this study uncover a comprehensive approach to monitoring compositional changes of hydrocarbon oxidation products in a spill event.

Environmental significance

The availability of new leases for petroleum production increases the risk of spills in high-latitude environments. Hydrocarbon oxidation products (HOPs), classified within operationally defined dissolved organic matter, are of emerging concern because they can be transported rapidly from the petroleum body and are undetectable by conventional gas chromatography-based methods, and information about their toxicity to aquatic organisms is limited. There are few reports on the pathways and chemical composition of HOPs formed by photochemical dissolution in high-latitude environments. Here we report quantitative and qualitative information about photochemically produced HOPs under simulated high-latitude conditions. Moreover, we report molecular signatures of classically defined naphthenic acids from photodissolution, a class of compounds known to be toxic to aquatic organisms.

1. Introduction

A response to oil spills at high latitudes is challenging due to complicated mechanical oil recovery techniques in icy environments. With the increase in petroleum development and the problematic nature of responding to high latitude spill events, it is imperative to understand the characteristics, transport, and fate of spilled oil in the Arctic and subarctic environments.[1]

Hydrocarbon oxidation products (HOPs) are degradation products of spilled oil. Once the oil enters the environment, it can undergo oxidation processes via microbial or photochemical activity to form HOPs.[2,3] The photochemical degradation

[a]Department of Chemistry, Chemical Analysis & Mass Spectrometry Facility, University of New Orleans, New Orleans, Louisiana 70148, USA. E-mail: mlharsha@uno.edu

[b]Pontchartrain Institute for Environmental Sciences, Shea Penland Coastal Education & Research Facility, University of New Orleans, New Orleans, Louisiana 70148, USA

[c]Department of Chemistry, University of Alaska Anchorage, Anchorage, Alaska 99508, USA

† Electronic supplementary information (ESI) available. See DOI: https://doi.org/10.1039/d2va00325b

© 2023 The Author(s). Published by the Royal Society of Chemistry

Environ. Sci.: Adv., 2023, 2, 447–461 | 447

process frequently involves aromatic compounds in the oil mixture reacting with light in the solar spectrum to produce HOPs.[4–6] HOPs in the environment can be mobilized through dissolution, which represents a threat to aquatic ecosystems and human health.[7] The dissolved fractions of the oxidized products are more mobile in aquatic environments and can be readily transported from the petroleum source.[8–16] HOPs can rapidly diffuse vertically and laterally in a water column. To fully understand all effects of an oil spill, including short- and long-term, it is critical to study the transport, concentration, and composition of dissolved HOPs. This information will allow for more informed decision-making for risk assessment and spill-response decisions.

HOPs and their petroleum parent compounds are challenging to characterize with traditional mass spectrometry techniques because the chemical composition of oil is complex, with over 100 000 identified molecular formulae, and they reside in the unresolved complex mixture.[14–16] Recent studies employed various complementary analytical techniques, such as gas chromatography-mass spectrometry (GC-MS), ultrahigh-resolution mass spectrometry (UHR-MS), etc., to address this knowledge gap.[14,17–23] This study utilizes complementary non-targeted and targeted techniques. Non-targeted analyses include two complementary analytical methods, LC-Orbitrap, to characterize the molecular-level composition and fluorescence excitation-emission matrix spectroscopy (EEMs) to characterize the optical properties of HOPs. The non-targeted techniques employed, LC-Orbitrap and EEMs, utilize similar fingerprinting type analyses that produce data, without a priori knowledge, that is further reduced into chemical "bins". The targeted analysis includes liquid chromatography – triple quadrupole mass spectrometry (LC-QQQ) to quantify a suite of commercially available oxyPAHs in HOPs generated from CI crude oil and diesel.[24] OxyPAHs are more water soluble and thus are potentially more bioavailable than PAHs.[25,26] This class of compounds is known to be toxic to the environment.[27–29] Another class of toxic compounds of interest is naphthenic acids (NAs). NAs are a well-studied fraction of an unresolved complex mixture known to be readily bioavailable and induce toxicological responses.[30–33] There is a significant body of literature on the chemical composition of NAs in oil sand produced water using various techniques, such as low resolution mass spectrometry[34] and UHR-MS (Fourier-transform ion cyclotron resonance,[35–37] time-of-flight,[38] and Orbitrap[37]), that characterize NAs as a wide spectrum of substituted carboxylic acids that are challenging to study. Although many studies report aliphatic acid photoproducts, information about the NA fraction of those acids from petroleum film photoproduction (oxidative formation and/or photo-enhanced dissolution) is limited.

Cook Inlet is a crucial watershed in Southcentral Alaska due to the major population centers surrounding it and commercial fishing, tourism, and diverse wildlife it supports. In addition, the region is an oil-producing basin with new lease sales and developments.[1] The Environmental Impact Statement (EIS) of the Cook Inlet oil and gas lease sale uses an oil weathering model (OWM) that assumes that a crude oil or diesel spill would be 1700–5100 bbls, occur at the surface or near-surface over a short period, and persist up to 30 days.[1] The OWM conditions allow spilled oil to be weathered into HOPs, which is acknowledged in the EIS, but no fate/transport models include this class of compounds. The routine analysis of petroleum compounds in Cook Inlet as aromatic hydrocarbons (benzene, toluene, ethylbenzene, and xylene (BTEX); polycyclic aromatic hydrocarbons (PAHs); and total petroleum hydrocarbons (TPH)) has occurred for the past 40 years.[1] Currently, there are no routine non-target analyses of the transport, fate, and impact of HOPs in Cook Inlet. The techniques outlined in this study can supplement existing analyses to more accurately understand the effects of an oil spill in Cook Inlet.

A previous study by Whisenhant et al. 2022 reports the molecular characterization of Alaska North Slope crude oil photo-oxidation products, herded burnt residue, and refined fuels, in natural water using UHR-MS and EEMs.[39] This study expands upon our prior findings by addressing a broader range of HOP subclasses (oxyPAH and naphthenic acids) and correlating non-target LC-Orbitrap and EEMs with targeted methods. This study is relevant to a more granular categorization of the HOPs formed from a potential spill event, which helps support environmental impact assessments in the many regions that have recently established HOP classification as a priority and urgent need. Such information can be helpful to support EIS development as high latitude oil and gas lease sales further expand. This study also reports a targeted analysis of HOPs and the molecular signatures of naphthenic acids in HOPs.

2. Materials and methods

2.1 Laboratory simulated oil spill

Laboratory simulated oil spills of CI crude oil (provided by Blue Crest Energy) and diesel (obtained by Shoreside Petroleum) were obtained using a solar simulator (Atlas Suntest XLS+). Diurnal temperature (12 °C) and sunlight exposure (250 W m^{-2}) of Cook Inlet in the summer were used.[40] Each oil substrate was added to artificial seawater (made with Instant Ocean Sea Salt at 36.86 g L^{-1} in Milli-Q water (18.2 MΩ cm)) at an oil load of 63.8 µL per 50 mL water in 100 mL thermostatically controlled jacketed beakers. Artificial seawater was used in this study to avoid background interference from dissolved organic matter or reactions from natural water. The composition of Instant Ocean Sea Salt has been previously reported and accurately represents the ionic strength of natural seawater.[41] Each jacketed beaker represents a single time point (irradiation period). There were four time points in the experiment, 1, 4, 7, and 10 days. Each time point for each oil substrate was analyzed in triplicate. Quartz lids were used to cover each beaker to reduce evaporation. An additional set of samples was incubated in the dark as a control to address any concerns about oxidation due to non-photolytic processes. Day 10 dark control samples for CI crude oil and diesel were completed on a larger scale of an oil load of 12.78 mL per 1000 mL of water to ensure that enough control substrate was produced for ultrahigh resolution mass spectrometry. After each exposure, water and oil were separated and

filtered through a 0.27 μm glass fiber filter pre-combusted at 550 °C and stored at −20 °C until analysis.

2.2 Dissolved organic carbon (DOC) analysis

Each sample was filtered through a pre-combusted (550 °C > 4 hours) Advantec GF-75 0.3 μm glass fiber filter into a pre-combusted amber glass vial. The pH of each sample was adjusted with high purity hydrochloric acid to pH < 2. Samples were stored in the dark and refrigerated (<4 °C) until they were ready for analysis. Samples were analyzed for DOC concentration with a Shimadzu TOC-V system equipped with an autosampler. DOC was measured as non-purgeable organic carbon converted to CO_2 and detected using a non-dispersive infrared detector.[42] DOC was calibrated with potassium hydrogen phthalate, and DOC standards were run regularly.

2.3 Excitation-emission matrix spectroscopy (EEMs)

The pH of the filtered samples was adjusted to pH 8 with NaOH for absorbance and fluorescence measurements with an Aqualog® fluorometer (Horiba Scientific, Kyoto, Japan).[43–45] Optical measurements were carried out in a 10 mm quartz cuvette in an excitation range from 240–800 nm in 5 nm increments and an emission range from 240–828.16 nm in 2.34 nm increments with an integration period of 1.5 s for light-exposed samples and 15 s for dark control samples. Each sample was diluted to an absorbance of 0.1 at 254 nm to reduce inner filter effects, using Milli-Q water (18.2 MΩ cm) to dilute.[46,47] Spectra were blank subtracted and corrected for instrument bias in excitation and emission prior to correction for inner filter effects. Fluorescence intensities were normalized to Raman scattering units and dilution corrected prior to PARAFAC analysis. The drEEM toolbox and MatLab code were utilized to complete PARAFAC of the EEMs.[48] The spectral properties of the resulting statistical model were validated by residual and split-half analysis.[49,50] The validated model was uploaded to the OpenFluor database to compare with published models above a 95% similarity score.[51]

2.4 LC-Orbitrap mass spectrometry

The filtrates from light exposed samples on days 4, 7, and 10 and dark control day 10 for CI crude oil and diesel were acidified to pH 2 and extracted via solid phase extraction (SPE) with Varian Bond Elut PPL cartridges (1 g, 6 mL).[52] SPE is an efficient method for isolating high-purity dissolved organic carbon extracts from the water-soluble fraction of oil.[53] The final concentrations of the extracts were adjusted to 500 μg C mL^{-1} to normalize carbon loads across samples to uncover compositional trends and stored at −20 °C before analysis.[52] Due to low DOC values and limited sample amounts in the dark samples, only day 10 of dark CI crude oil and diesel underwent LC-Orbitrap analysis. Specific instrument parameters are reported in the ESI.†

Collected mass spectra were co-added across the chromatogram and internally recalibrated with a "walking" calibration equation, followed by a blank subtraction and molecular formula assignment (C4-50, H4-100, O1-40, N0-2, and S0-1) with Composer software (Sierra Analytics). Molecular formula assignment constraints were based on Hawkes et al. 2020, including double bond equivalents minus oxygen (DBE − O) ≤ 10, O/C ≤ 1.2, 0.3 ≤ H/C ≤ 2.2, and Kendrick mass defect (KMD) ≤ 0.4 or ≥ 0.9.[54] Molecular formulae were classified based on stoichiometry into the following categories: condensed aromatic (CA) (modified aromaticity index (AI_{mod}) ≥ 0.67), aromatic (0.67 > AI_{mod} ≥ 0.5), unsaturated low oxygen (ULO) (AI_{mod} < 0.5, H/C < 1.5, O/C < 0.5), unsaturated high oxygen (UHO) (AI_{mod} < 0.5, H/C < 1.5, O/C ≥ 0.5), aliphatic (H/C ≥ 1.5), and classically defined naphthenic acids ($C_nH_{2n+z}O_2$ in which n is the number of carbon atoms and Z is zero or a negative even number that represents hydrogen deficiency, and exclusion rules reported by Holowenko et al. 2002 to eliminate carbon number groups and Z family values that do not conform to the empirical formula).[34,55–59]

2.5 Targeted analysis of OxyPAHs and PAHs

Eight oxyPAHs and 24 PAHs were chosen for the targeted analysis of oxyPAHs and PAHs in HOPs formed from CI crude oil and diesel. The oxyPAH compounds were 1-naphthol, 2-naphthol, phenanthrenequinone, 1,4-anthraquinone, 1-hydroxy-9,10-anthraquinone, 1,4-chrysenequinone, 5,12-naphthacenequinone and benzanthraquinone. The PAH compounds were naphthalene, acenaphthylene, 1-methylnaphthalene, 2-methylnaphthalene, acenaphthene, fluorene, 9-methyl-9H-fluorene, phenanthrene, 2,6-dimethylnaphthalene, anthracene, fluoranthene, 2,3,6-trimethylnaphthalene, 9-methylanthracene, pyrene, 9,10-dimethylanthracene, 1-methylpyrene, benz(a)anthracene, chrysene, benzo(a)pyrene, benzo(b)fluoranthene, benzo(k)fluoranthene, benzo(ghi)perylene, dibenzo(ah)anthracene, and indenopyrene.

The aqueous filtrate of the dissolved phase from CI crude oil and diesel experiments was added into different separatory funnels, and deuterated PAH surrogates (Table S10†) were added to the filtrate to make a 1 μg L^{-1} concentration. Liquid–liquid extraction was performed three times with 20 mL of 9 : 1 chloroform : tetrahydrofuran (THF) as a solvent and anhydrous Na_2SO_4 as a drying agent for the organic layer. A liquid–liquid extraction procedure was optimized as extraction recoveries using dispersive liquid–liquid micro extractions reported in the literature were not reproducible.[60] During optimization, chloroform yielded higher extraction recoveries for both PAHs and oxyPAHs when compared to ethyl acetate and dichloromethane; further addition of THF as a dispersive solvent to increase chloroform-artificial sea water biphase interaction improved oxyPAH extraction efficiency. Approximately 60 mL of the organic extract was evaporated to 0.1 mL under N_2 at 25 °C. 5 μL of 10 μg mL^{-1} deuterated PAH internal standard solution was added. Each extract was then reconstituted in 10 mL of methanol before being evaporated to 1 mL. Finally, the extracts were filtered through a 0.2 μm nylon filter and stored −20 °C until analysis. Average recoveries ($n = 6$) were 69.3 ± 13.6–88.4 ± 15.2% and 89.7 ± 6.9–125.4 ± 26.0% for oxyPAHs and PAHs, respectively, with the exception of anthraquinone (24.8 ± 7.7%) and 1,4-chrysenequinone (5.8 ± 1.8%) which were ineffectively

© 2023 The Author(s). Published by the Royal Society of Chemistry

Environ. Sci.: Adv., 2023, **2**, 447–461 | **449**

recovered by this method (Table S6†). To our knowledge, no previous studies report higher recoveries for oxyPAHs.[24]

3. Results and discussion

3.1 Photoproduction of HOPs

The concentration of DOC is positively correlated with light exposure time (Pearson correlation coefficient, $r_{crude} = 0.90$ and $r_{diesel} = 0.92$) (Fig. 1). CI crude oil and diesel samples exposed to light resulted in higher DOC than dark samples ($p < 0.05$ (one-way ANOVA)) (Table S1†). Only minor changes in the DOC concentrations of dark samples are attributed to readily available water-soluble compounds in petroleum.[61] As time increases, the water-soluble compounds in petroleum can partition into the aqueous phase, resulting in a small increase in DOC.

Light-exposed diesel initially produced higher DOC on days 1 and 4 compared to CI crude oil, where CI crude oil produced more DOC on days 7 and 10. Diesel is a refined fuel that consists of C8–C21 compounds distilled from crude oil. This character can make it more readily photosolubilized compared to whole crude oil.[23] These results match those in a report by Zito et al. 2019 that showed that DOC concentrations produced from a relatively light crude oil increased more rapidly at early irradiation periods. Still, with extended exposure, the DOC from the light crude oil plateaued while that from heavy fuel oil continued to increase.[13]

3.2 Optical characterization of HOPs

Optical spectroscopy is employed to uncover changes in chromophore composition in HOPs. Table S2† reports the spectral indices of the fluorescent dissolved organic matter found in HOPs from each sample. The humification index (HIX) is of particular interest in uncovering compositional trends in HOPs, as it is a general indicator of aromaticity and oxygen content.


Fig. 1 Temporal shifts in DOC for HOPs in all samples. ($N = 3$, $\pm$ SD).

HIX is derived from the intensity of emission within the ranges of 435–480 nm and 300–345 nm with an excitation wavelength of 254 nm.[62] As HIX increases, the ratio of hydrogen to carbon decreases and oxygen content increases.[47,62] Increasing HIX values represent the relative increase in long-wavelength, "humified", water-soluble, oxidized compounds and decrease in short-wavelength compounds. HOPs formed from CI crude oil range in HIX values from 0.58 ± 0.03 at day 1 to 0.66 ± 0.01 at day 10, and HOPs created from diesel range from 0.36 ± 0.02 at day 1 to 0.20 ± 0.01 at day 10. The inverse relationship between the two fuel types suggests that HOPs formed from CI crude oil are more aromatic and oxygenated as time increases. In contrast, HOPs formed from diesel become less aromatic and oxygenated as time increases. Aromaticity and oxygenation trends in diesel and CI crude oil are further explored through non-target molecular characterization techniques discussed later in this study. This relationship can be attributed to compositional differences in the parent petroleum. Crude oil consists of relatively higher molecular weight and aromatic compounds relative to diesel.[63]

Specific UV absorbance at 254 nm (SUVA$_{254}$) is another optical parameter of interest for tracking compositional changes in HOPs as it measures the amount of light absorbing dissolved organic matter. SUVA$_{254}$ is calculated by dividing absorbance at 254 nm (a_{254}) by the DOC concentration (a_{254} m^{-1}/DOC mg L^{-1}). SUVA$_{254}$ values track compositional changes in HOPs through aromaticity. Increasing SUVA$_{254}$ after light exposure for both fuel types suggests that aromatic HOPs are produced.[64] CI crude oil and diesel exposed to light varied in maximum SUVA$_{254}$ (Table S1†). CI crude oil SUVA$_{254}$ ranged between 0.0100 ± 0.005 (day 1) and 0.0169 ± 0.001 L mg^{-1} cm^{-1} (day 10). Diesel SUVA$_{254}$ ranged between 0.0108 ± 0.001 (day 1) and 0.0139 ± 0.001 L mg^{-1} cm^{-1} (day 4). The temporal difference of SUVA$_{254}$ maxima for CI crude oil and diesel suggests compositional differences in the photoproduction of HOPs from different fuel sources and time points, which is explored further in detail in this experiment. CI crude oil maximum SUVA$_{254}$ at day 10 suggests that aromatic HOPs are produced throughout the total irradiation time, supported by increasing HIX values. Diesel maximum SUVA$_{254}$ on day 4 indicates a decrease in aromatic HOP production after day 4, which, combined with increasing DOC after day 4, suggests that relatively aliphatic HOPs are produced from days 4–10. These results are consistent with reduced HIX values as both indicate relative loss in aromaticity and could allude to photo-degradation of small aromatic molecules to aliphatic-like features. The Whisenhant et al. 2022 study, utilizing high-latitude irradiation conditions, follows similar values for both crude oil (0.009 (day 1)–0.015 L mg^{-1} cm^{-1} (day 10)) and diesel (0.011 (day 1)–0.012 L mg^{-1} cm^{-1} (day 10)).[39] These combined results illustrate that the photoproduction of diverse compositional HOPs occurs when CI crude oil and diesel are exposed to light.

Parallel factor (PARAFAC) analysis was used to uncover underlying fluorescence components present in the EEMs dataset, allowing for an optical index for tracking compositional changes through the production of HOPs over time. A validated

450 | Environ. Sci.: Adv., 2023, 2, 447–461

© 2023 The Author(s). Published by the Royal Society of Chemistry
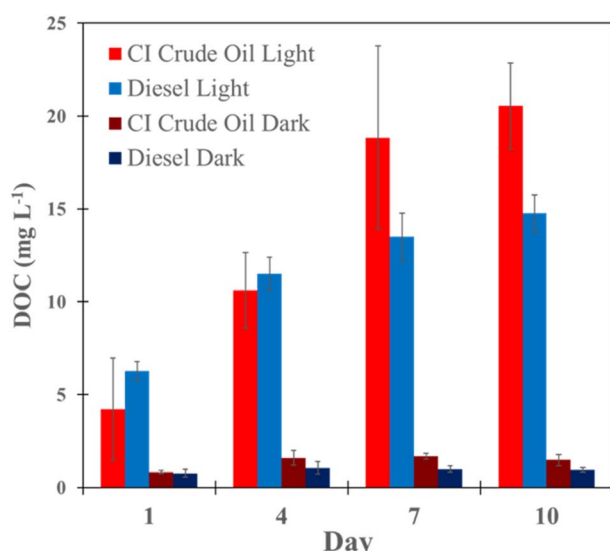
six-component PARAFAC model was derived from the EEMs (Fig. 2a and S1†). Component 1 (C1) had excitation and emission (Ex/Em) maxima of 240/374 nm and did not match any other components in the OpenFluor database (>95% similarity score), suggesting that a unique HOP signature is present. Although there were no matches in the OpenFluor database for C1, Ex/Em spectra with similar wavelengths are reported for petroleum degradation products and NAs.[65,66] Component 2 (C2 Ex/Em 260/376 nm) (matched a 97% similarity score) is consistent with a previous report by Zito *et al.* (2019), indicating a petroleum-derived DOM signal produced from irradiating heavy and light oils from a surrogate Macondo oil (light) produced after 24 hours.[13] These results show that C2 from this study is indicative of HOP fluorescent signatures. Component 3 (C3 Ex/Em 270/294 nm), Component 4 (C4 Ex/Em 280/340 nm), and Component 6 (C6 Ex/Em 240/320 nm) matched three, five, and seven entries in the OpenFluor database, respectively. These components are called "tyrosine-like" and "tryptophan-like" ("protein-like) fluorescent signatures in the organic biogeochemistry community.[13,67–73] However, there are no proteins or amino acids in petroleum. Rather, these fluorescence signatures correspond with relatively reduced (aliphatic, low heteroatom) HOPs.[8,74,75] Moreover, there are reports of similar fluorescence signatures from water-soluble aliphatic acid photo-oxidation products produced from irradiated oil films and NA standard mixtures.[76,77] Component 5 (C5 Ex/Em 250/460 nm) matched with seven components representing "terrestrial humic-like" fluorescence in a range from 95–96% OpenFluor similarity score.[78–84]

Contributions of each component in all samples are reported in Table S3.† Principal component analysis shows the relationship between each component and the samples (Fig. 2a). CI crude oil light samples positively correlate with C1, C2, and C5. Days 4 and 7 are closely related to C2 and C1, respectively, which are the two petroleum unique components, with C1 being unique to this study (no matches in OpenFluor above). For the CI crude, day 10 is closely related to C5 or the "humic-like" fluorescence that suggests more aromaticity and oxygenation, which aligns with the photodissolution of petroleum. Another interesting relationship is between C4 and C3 and the amount of time diesel is irradiated with light (Fig. 2b). C3 represents the production of HOPs, and C4 represents the degradation of parent petroleum compounds. These results show that fluorescent signatures can accurately monitor temporal and compositional changes in HOPs.

The HIX values, SUVA$_{254}$ values, and PARAFAC model show a cohesive description of the chemical composition of HOPs formed from CI crude oil and diesel. HOPs produced from CI crude oil are more oxygenated and aromatic in nature, correlating with increasing HIX, increasing SUVA$_{254}$, and long-wavelength "humic-like" fluorescence (C1, C2, and C5). HOPs produced from diesel are more reduced and aliphatic, correlating with decreasing HIX, decreasing SUVA$_{254}$, and short-wavelength "protein-like" fluorescence (C3, C4, and C6). Optical characterization emphasizes the compositional changes and temporal trends in the formation of HOPs from different petroleum sources.

3.2.1 Molecular characterization of HOPs. Molecular-level characterization is utilized to further understand the composition of HOPs and complement the optical characterization results. Liquid chromatography (LC)-Orbitrap mass spectrometry was used to characterize the molecular composition of days
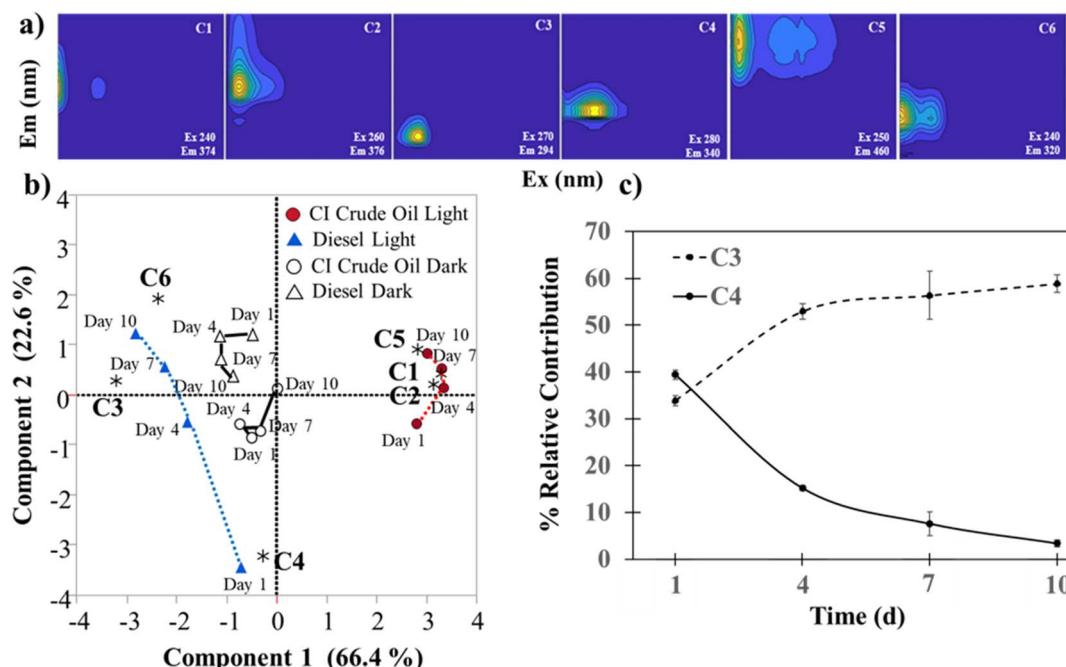

Fig. 2 (a) PARAFAC components (b) PCA biplot, loadings represent PARAFAC components. (c) Temporal relationship between C3 and C4 in HOPs formed from light irradiated diesel. ($N = 3$, $\pm$ SD).
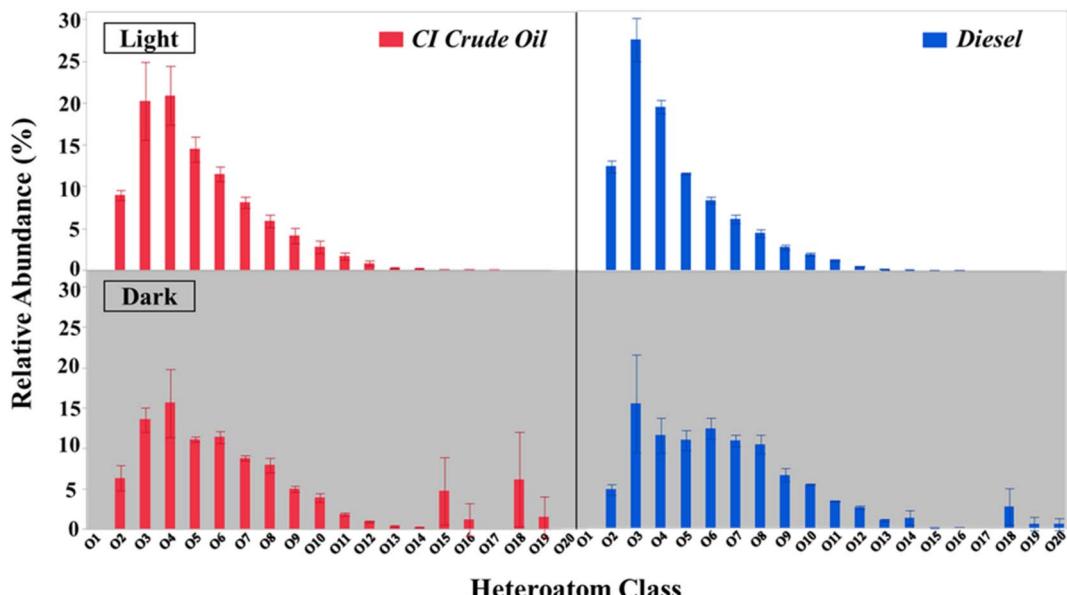
Fig. 3 Heteroatom oxygen class graphs from day 10 samples, CI crude oil (red), diesel (blue), irradiated (top), and dark (bottom). ($N = 3$, $\pm$ SD).

4, 7, and 10 sunlight-irradiated CI crude oil and diesel. Heteroatom oxygen class composition uncovers trends in oxygenation (Fig. 3). CI crude oil and diesel derived HOPs are composed of compounds that have 2–17 and 2–16 oxygens per molecule, respectively. The most abundant species in CI crude oil derived HOPs and CI crude oil dark control are in the O_4 class. Diesel derived HOPs and diesel dark controls have the most abundant species in the O_3 class. Dark control samples express the composition of the water-soluble fraction of parent petroleum. The water-soluble compounds from parent petroleum (dark control samples) are composed of compounds that have 2–20 oxygens per molecule. Low concentrations of these compounds can be attributed to the low abundance of polar, water-soluble compounds found in parent petroleum.[85]

A van Kravelen diagram can be used to better characterize HOPs in terms of their molecular composition (Fig. 4).[86] The dots on the plot represent unique molecular features assigned from mass spectral data with the same O/C and H/C ratios.[57] The diagram can be further decomposed into discrete molecular classification regions (CA, aromatic, ULO, UHO, and
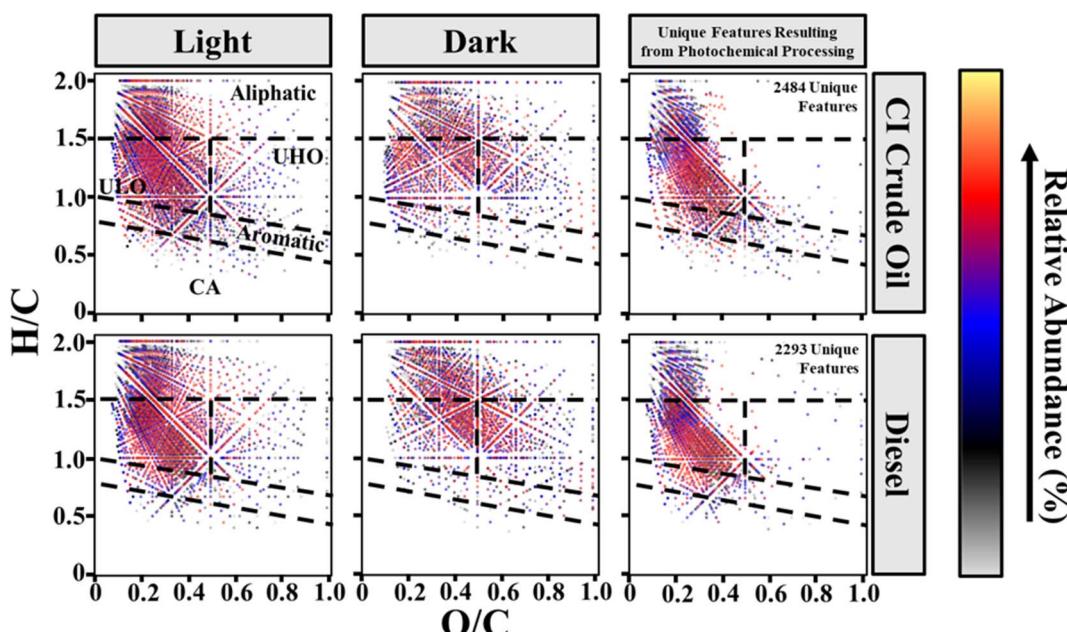

Fig. 4 Van Krevelen subtraction plots of day 10 dark and light treatments for CI crude oil and diesel where each data point represents a unique molecular feature. Photochemical processing of CI crude oil results in 2484 unique features and diesel results in 2293 unique features.

aliphatic). Van Krevelen diagrams can also highlight molecular compositional differences between the petroleum source and illumination through a subtraction plot (Fig. 4). There are 2483–2492 and 1986–2293 unique features resulting from photochemical processing of CI crude oil and diesel derived HOPs, respectively (Table S5†). The unique photochemical features mainly consist of aliphatic (19.21 ± 6.24–$35.26 \pm 20.38\%$ relative abundance), ULO (48.01 ± 15.10–$65.14 \pm 4.95\%$ relative abundance), and aromatic (9.93 ± 0.49–$15.94 \pm 2.17\%$ relative abundance) molecular classifications (Table S5†). The molecular composition classifications of HOPs reveal that relatively reduced, saturated, and aromatic compounds are produced by sunlight in high-latitude environments from both CI crude and diesel. CI crude oil and diesel derived HOPs featuring relatively low oxygenated maximum abundance species (O_4 and O_3, respectively) support that relatively reduced compounds are produced.

Principal component analysis between composition class contributions (Table S4†), fuel types, and illumination period was conducted to gain a better understanding of the composition and temporal changes in HOPs (Fig. 5). Day 4 light irradiated CI crude oil and diesel produced the highest relative abundances of CA compounds, 4.89 ± 0.17 and $3.07 \pm 0.30\%$, and aromatic compounds, 11.32 ± 0.37 and $9.46 \pm 0.96\%$, respectively. Day 7 light irradiated CI crude oil and day 10 diesel produced the highest relative abundance of ULO compounds, 47.23 ± 2.05 and $48.61 \pm 2.05\%$, respectively. Irradiated CI crude oil HOPs consist of slightly more condensed aromatic and aromatic compounds, whereas light irradiated diesel HOPs consist of marginally more ULO compounds. Dark controls for CI crude oil and diesel produced the highest abundance of UHO compounds, 19.18 ± 1.48 and $21.21 \pm 2.03\%$, respectively, and aliphatic compounds, 39.80 ± 0.75 and $46.11 \pm 1.81\%$, respectively.
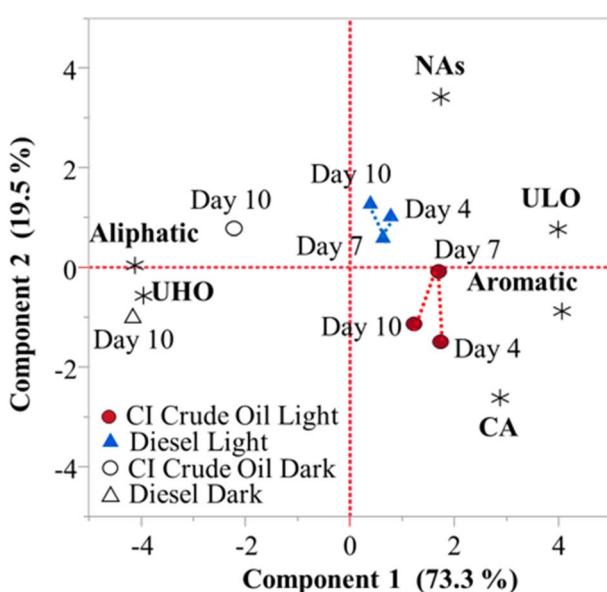
Fig. 5 PCA biplot, loadings represent molecular classifications.

Aliphatic and UHO groups are closely related to the dark samples, while CA, aromatics, NAs, and ULO groups are closely related to the light samples. These trends are consistent with the compositional changes induced by illumination of crude and diesel fuels recently observed with an UHR-MS by Whisenhant et al. (2022). The dark samples consisted of aliphatic and UHO groups due to the readily available water-soluble compounds that the parent petroleum contains.[61] HOPs formed from CI crude oil consisted of more aromatic and CA compounds, whereas HOPs formed from diesel are more aliphatic. Differences between CI crude oil and diesel-produced HOPs come from the compositional differences between the parent petroleum sources.[5] The molecular characterization data express that dark control samples (representatives of the water soluble compounds in petroleum) are more oxygenated and aliphatic than HOPs. The data also show that HOPs generated from CI crude oil are more aromatic and oxygenated than HOPs generated from diesel, which verifies the results from the optical studies (HIX, SUVA$_{254}$, and PARAFAC).

Although this study focused primarily on photodegradation, it is important to draw comparisons between other major weathering processes, such as biodegradation. Biodegradation of petroleum consists of two major pathways: first, an aerobic process, including enzyme mediated metabolism and biosynthesis and second, an anoxic process, including anaerobic processes such as fumarate addition, oxygen independent hydroxylation, and/or carboxylation which forms HOPs.[87–92] The pathways of abiotic vs. biotic degradation are both dependent on the specific petroleum composition and the environmental conditions of a spill. Some compound classes such as aromatic hydrocarbons are known to be more sensitive to photodegradation, where saturated hydrocarbons have been shown to be more susceptible to biotic pathways.[93–99] Podgorski et al. (2021) examined the biodegradation of oil contaminated groundwater, finding HOPs to exhibit lower relative abundances of condensed aromatics, aliphatics, and unsaturated low oxygen compounds accompanied by an increase in unsaturated high oxygen compounds and no significant temporal changes in aromatics.[75] Biodegradation products in general are less aromatic (2.39–3.57%)[75] with more UHO (15.5–45.1%)[75] than the photodegradation products we observed in this study (aromatic: 8.15–11.32%, UHO: 6.63–8.81%). Aliphatic hydrocarbons are the most bio-labile class of petroleum.[93,95,100] However, both biotic and abiotic pathways are relevant, with the relative pathway contributions being driven by seasonal environmental factors such as temperature, redox potential, water quality, transmittance of light into the water column, and others.

3.2.2 Molecular signatures of naphthenic acids. Formula classification assignments for petroleum water-soluble photoproducts do not generally include NAs as a compound class. Recent studies report the photochemical formation of naphthenic acids in simulated petroleum spills over water.[101,102] Due to their ecotoxicological significance, we measured the occurrence of water-soluble NAs produced from CI crude oil and diesel under high latitude conditions. NAs were detected and identified from molecular formula assignments based on

© 2023 The Author(s). Published by the Royal Society of Chemistry

Environ. Sci.: Adv., 2023, **2**, 447–461 | **453**

stoichiometry $C_nH_{2n+z}O_2$ by utilizing exclusion rules reported by Holowenko et al. 2002.[56] It is acknowledged that this operational definition may not disambiguate NAs from polycyclic aromatic diketones and dialdehydes with long alkyl side chains or some photo-oxidative cleavage products.[103,104] The relative abundance of NAs produced from CI crude oil ranges from 1.78 ± 0.35% (light day 10) to 1.95 ± 0.10% (dark day 10) and diesel ranges from 1.66 ± 0.13% (dark day 10) to 1.96 ± 0.10% (light day 4). In general, no temporal trends in NA production were noted (i.e. between irradiated and dark groups).

Water-soluble naphthenic acid composition varied between irradiated CI crude oil and diesel (Fig. S2†). NAs produced in this study were composed of compounds between 9 and 25 carbons with Z values corresponding to structural composition ($Z = 0$ acyclic, $Z = -2$ one ring, $Z = -4$ two rings, etc.). The most abundant NAs found in non-irradiated (dark) controls contained carbon numbers between 13 and 18, and $Z = -12–0$. This represents a wide variety of compounds that range from highly branched aliphatic carboxylic acids to complex aromatic ring systems with up to six rings. Irradiated (light-exposed) NAs on the other hand contained predominantly 9–13 carbons with $Z = -6–0$. This indicates that photo-oxidation may select for NAs with lower molecular weights (lower carbon numbers) and a higher degree of saturation (larger Z family value). Recent studies have similarly noted an increase in low carbon numbers and high Z family values after irradiation of petroleum sources.[101,102] Interestingly, the structures of NAs produced from irradiation are more diverse than NAs from parent petroleum sources (Fig. 6). Temporally, the relative abundance of NAs with carbon numbers 9–12 and 21–24 increased, accompanied by a decrease in carbon numbers between 15 and 19 in diesel and CI crude oil derived HOPs (Fig. 6).

Previous studies on NA toxicity found that low molecular weight NAs induce a higher toxicological response than high molecular weight NAs.[30,56,105] NAs in HOPs are of toxicological concern because an etiological agent at 50–500 µg L^{−1} can induce sublethal endpoints such as endocrine disruption,[106–108]

increased oxidative stress,[109,110] liver toxicity,[111] and disruption of energy pathways.[33] This process of photoproduction of NAs in HOPs from CI crude oil and diesel has, to the best of our knowledge, not been reported previously, and the dose-response relationship of NAs merits further consideration.[30,112–117]

3.3 Detection of oxyPAHs and PAHs in HOPs

A targeted analysis was employed to further understand the composition of HOPs formed through CI crude oil and diesel. LC-QQQ provided quantitation of 8 oxyPAHs, which were correlated to the analysis of 24 PAHs in light-treated samples on days 1, 4, 7, and 10. The oxyPAHs targeted in this analysis consisted of heteroatom oxygen classes between O1–O3. Characterization and quantification of lower oxygenated compounds are of great interest due to their toxicity and abundance in HOPs. Two oxyPAH compounds and 11 PAH compounds were detected (Table S6†). The oxyPAHs phenanthrenequinone and 1,4-anthraquinone were present in light-treated CI crude oil HOPs at concentrations of 0.11 ± 0.10 (day 7)–0.13 ± 0.11 (day 10) and 0.14 ± 0.12 (day 4)–0.21 ± 0.01 (day 10) µg L^{−1}, respectively. OxyPAHs were not detected in the irradiated diesel samples. Acenaphthene is a diesel-unique PAH with no detection in irradiated CI crude oil samples. Anthracene is a CI crude oil unique PAH, with no detection in irradiated diesel samples. The other nine PAH compounds were detected in light-treated CI crude oil and diesel HOPs.

There is an inverse relationship between the oxyPAH, phenanthrenequinone, and its associated PAH, phenanthrene, in irradiated CI crude oil ($p < 0.05$ (one-way ANOVA)) (Fig. 7a). Phenanthrene degrades over time, while phenanthrenequinone is produced. This relationship is consistent with the photooxidation of a PAH to its respective oxyPAH. 1,4-anthraquinone and anthracene do not have a statistically significant relationship ($p > 0.05$ (one-way ANOVA)). However, 1,4-anthraquinone is strongly positively correlated with the amount of time irradiated ($r = 0.87$), suggesting that 1,4-anthraquinone is produced over
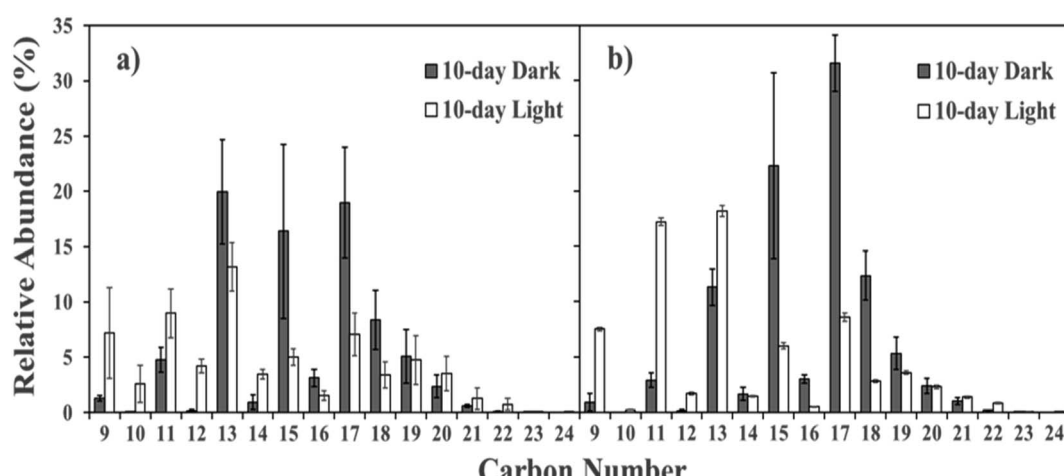
Fig. 6 Relative abundance (within the naphthenic acid classification) of each carbon number in (a) CI crude oil and (b) diesel at day 10. ($N = 3, \pm$ SD).

© 2023 The Author(s). Published by the Royal Society of Chemistry
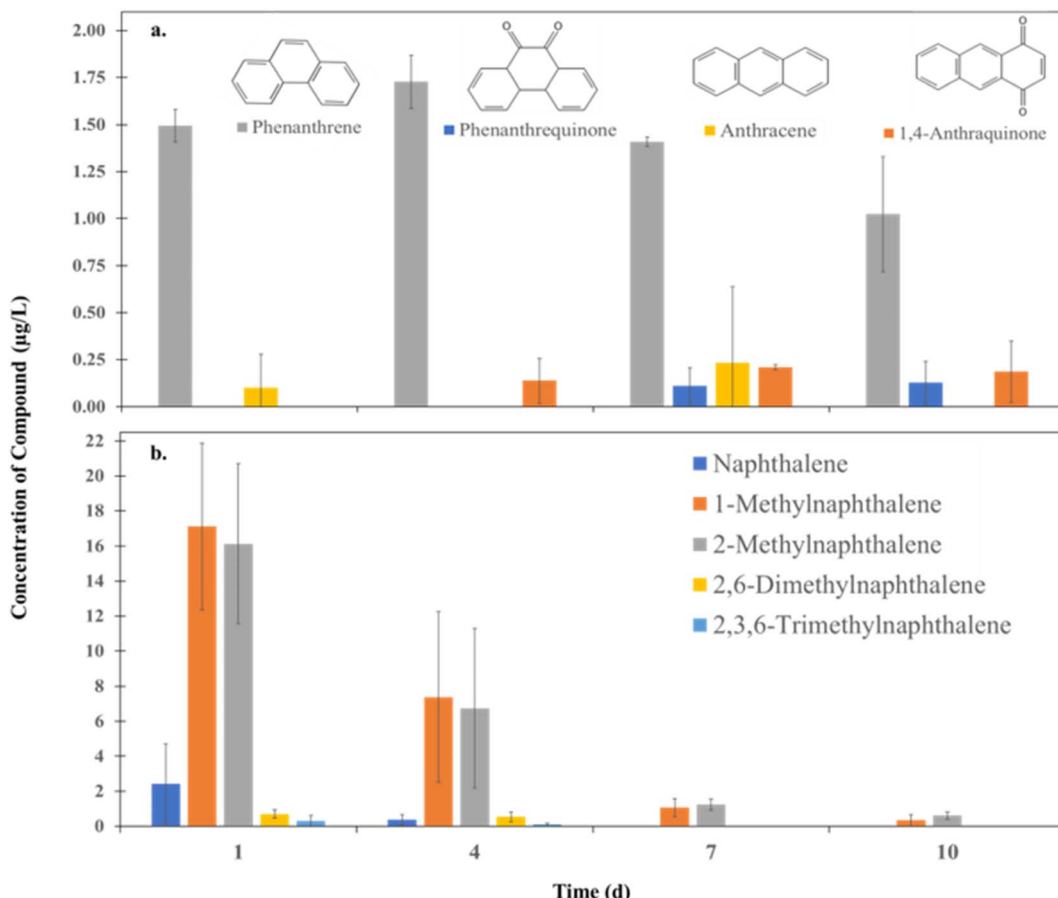
Fig. 7 (a) Oxy-PAHs and their respective PAH derivatives and (b) methylated naphthalene concentrations in HOPs formed from irradiated CI crude oil. ($N = 3$, $\pm$ SD).

time. This relationship aligns with more oxidized species being produced with longer irradiation times. Transformations of PAHs into oxyPAHs have been previously reported through photochemical processes.[28,118,119] Phenanthrenequinone/ phenanthrene and 1,4-anthraquinone have potential use for tracking overall degradation and compositional changes in an oil spill event.

Another interesting class of compounds that could be used for monitoring in a spill event is methylated naphthalenes. The concentration of naphthalene-type compounds over time in irradiated CI crude oil can be seen in Fig. 7b. The concentration of 1- and 2-methylnaphthalene was greater than the concentration of naphthalene following irradiation of CI crude oil, suggesting that single substituted methylated naphthalenes may be more useful for monitoring CI crude oil dissipation. Future work should include methylated oxyPAHs due to the potential prevalence of other methylated PAHs. Furthermore, methylated PAHs produce transient radical reactive species with relatively greater stability than non-substituted congeners, which may increase the formation of oxidized products. Current efforts include development of a data-dependent tandem mass spectrometry method utilizing MS2 fragmentation to detect additional oxyPAH congeners.

OxyPAHs are a class of compounds that are commonly missed in traditional TPH analysis.[120] The reported results expand on traditional TPH methods by identifying two specific oxyPAHs in crude oil and emphasizing the mixture's complexity due to methylated homologues in both fuel types. Although the list of oxyPAHs and PAHs used in this study is not comprehensive of all the compounds in HOPs formed from CI crude oil and diesel, some promising compounds and relationships can be used to track compositional changes of HOPs for a cheaper and more routine analysis.

4. Conclusions

This study identifies HOP formation resulting from irradiation of both crude oil and diesel over seawater using simulated environmental conditions of the sub-Arctic. DOC measurements confirmed that sunlight irradiation mobilizes petrogenic carbon into seawater. Six unique fluorescence EEM components were identified in irradiated HOPs, ranging from reduced to oxidized signatures. Irradiated seawater produced greater abundances of CA, aromatic, and ULO chemical features and higher oxyPAH loads predominated by phenanthrenequinone and 1,4-anthraquinone. Naphthenic acid production was driven by a decrease in the molecular weight and an increase in

© 2023 The Author(s). Published by the Royal Society of Chemistry

Environ. Sci.: Adv., 2023, **2**, 447–461 | **455**

saturation after irradiation. While the toxicological significance of HOPs is still an emerging research area, the production of naphthenic acids and oxyPAHs, which this study identifies, could have important toxicological implications during an oil spill event in high-latitude regions.

Author contributions

Conflicts of interest

There are no conflicts to declare.

Acknowledgements

References

1 Bureau of Ocean Energy Management, *Alaska Outer Continental Shelf Cook Inlet Planning Area Oil and Gas Lease Sale 244*, Final Environmental Impact Statement, 2016.

2 C. Aeppli, C. A. Carmichael, R. K. Nelson, K. L. Lemkau, W. M. Graham, M. C. Redmond, D. L. Valentine and C. M. Reddy, Oil Weathering after the Deepwater Horizon Disaster Led to the Formation of Oxygenated Residues, *Environ. Sci. Technol.*, 2012, **46**, 8799–8807.

3 N. Fry and R. A. Steenson, *User's Guide: Derivation and Application of Environmental Screening Levels (ESLs), San Francisco Bay Regional Water Quality Control Board: San Fransisco*, 2019, 1–35.

4 M. D'Auria, L. Emanuele, R. Racioppi and V. Velluzzi, Photochemical degradation of crude oil: Comparison between direct irradiation, photocatalysis, and photocatalysis on zeolite, *J. Hazard. Mater.*, 2009, **164**, 32–38.

5 P. Zito, H. Chen, D. C. Podgorski, A. M. McKenna and M. A. Tarr, Sunlight creates oxygenated species in water-soluble fractions of Deepwater horizon oil, *J. Hazard. Mater.*, 2014, **280**, 636–643.

6 C. P. Ward, C. M. Sharpless, D. L. Valentine, D. P. French-McCay, C. Aeppli, H. K. White, R. P. Rodgers, K. M. Gosselin, R. K. Nelson and C. M. Reddy, Partial Photochemical Oxidation Was a Dominant Fate of Deepwater Horizon Surface Oil, *Environ. Sci. Technol.*, 2018, **52**, 1797–1805.

7 C. D. Johnston and M. G. Trefry, Characteristics of light nonaqueous phase liquid recovery in the presence of fine-scale soil layering, *Water Resour. Res.*, 2009, **45**, W05412.

8 J. Brünjes, M. Seidel, T. Dittmar, J. Niggemann and F. Schubotz, Natural Asphalt Seeps Are Potential Sources for Recalcitrant Oceanic Dissolved Organic Sulfur and Dissolved Black Carbon, *Environ. Sci. Technol.*, 2022, **56**, 9092–9102.

9 D. H. Freeman and C. P. Ward, Sunlight-driven dissolution is a major fate of oil at sea, *Sci. Adv.*, 2022, **8**, eabl7605.

10 H. Maki, T. Sasaki and S. Harayama, Photo-oxidation of biodegraded crude oil and toxicity of the photo-oxidized products, *Chemosphere*, 2001, **44**, 1145–1151.

11 M. Tarr, P. Zito, E. Overton, G. Olson, P. Adhikari and C. Reddy, Weathering of Oil Spilled in the Marine Environment, *Oceanography*, 2016, **29**, 126–135.

12 C. P. Ward and E. B. Overton, How the 2010 Deepwater Horizon spill reshaped our understanding of crude oil photochemical weathering at sea: a past, present, and future perspective, *Environ. Sci.: Processes Impacts*, 2020, **22**, 1125–1138.

13 P. Zito, D. C. Podgorski, J. Johnson, H. Chen, R. P. Rodgers, F. Guillemette, A. M. Kellerman, R. G. M. Spencer and M. A. Tarr, Molecular-Level Composition and Acute Toxicity of Photosolubilized Petrogenic Carbon, *Environ. Sci. Technol.*, 2019, **53**, 8235–8243.

14 G. S. Frysinger, R. B. Gaines, L. Xu and C. M. Reddy, Resolving the Unresolved Complex Mixture in Petroleum-Contaminated Sediments, *Environ. Sci. Technol.*, 2003, **37**, 1653–1662.

15 L. C. Krajewski, R. P. Rodgers and A. G. Marshall, 126 264 Assigned Chemical Formulas from an Atmospheric Pressure Photoionization 9.4 T Fourier Transform Positive Ion Cyclotron Resonance Mass Spectrum, *Anal. Chem.*, 2017, **89**, 11318–11324.

16 D. C. Palacio Lozano, R. Gavard, J. P. Arenas-Diaz, M. J. Thomas, D. D. Stranz, E. Mejía-Ospino, A. Guzman, S. E. F. Spencer, D. Rossell and M. P. Barrow, Pushing the analytical limits: new insights into complex mixtures using mass spectra segments of constant ultrahigh resolving power, *Chem. Sci.*, 2019, **10**, 6966–6978.

17 G. Isaacman, K. R. Wilson, A. W. H. Chan, D. R. Worton, J. R. Kimmel, T. Nah, T. Hohaus, M. Gonin, J. H. Kroll, D. R. Worsnop and A. H. Goldstein, Improved Resolution of Hydrocarbon Structures and Constitutional Isomers in Complex Mixtures Using Gas Chromatography-Vacuum Ultraviolet-Mass Spectrometry, *Anal. Chem.*, 2012, **84**, 2335–2342.

18 A. M. McKenna, R. K. Nelson, C. M. Reddy, J. J. Savory, N. K. Kaiser, J. E. Fitzsimmons, A. G. Marshall and R. P. Rodgers, Expansion of the Analytical Window for Oil Spill Characterization by Ultrahigh Resolution Mass Spectrometry: Beyond Gas Chromatography, *Environ. Sci. Technol.*, 2013, **47**, 7530–7539.

19 S. F. Niles, M. L. Chacón-Patiño, H. Chen, A. M. McKenna, G. T. Blakney, R. P. Rodgers and A. G. Marshall, Molecular-Level Characterization of Oil-Soluble Ketone/Aldehyde Photo-Oxidation Products by Fourier Transform Ion Cyclotron Resonance Mass Spectrometry Reveals Similarity Between Microcosm and Field Samples, *Environ. Sci. Technol.*, 2019, **53**, 6887–6894.

20 B. M. Ruddy, C. L. Hendrickson, R. P. Rodgers and A. G. Marshall, Positive Ion Electrospray Ionization Suppression in Petroleum and Complex Mixtures, *Energy Fuels*, 2018, **32**, 2901–2907.

21 B. M. Ruddy, M. Huettel, J. E. Kostka, V. V. Lobodin, B. J. Bythell, A. M. McKenna, C. Aeppli, C. M. Reddy, R. K. Nelson, A. G. Marshall and R. P. Rodgers, Targeted Petroleomics: Analytical Investigation of Macondo Well Oil Oxidation Products from Pensacola Beach, *Energy Fuels*, 2014, **28**, 4043–4050.

22 S. A. Wise, R. P. Rodgers, C. M. Reddy, R. K. Nelson, E. B. Kujawinski, T. L. Wade, A. D. Campiglia and Z. Liu, Advances in Chemical Analysis of Oil Spills Since the Deepwater Horizon Disaster, *Crit. Rev. Anal. Chem.*, 2022, 1–60, DOI: 10.1080/10408347.2022.2039093.

23 P. Zito, D. C. Podgorski, T. Bartges, F. Guillemette, J. A. Roebuck, R. G. M. Spencer, R. P. Rodgers and M. A. Tarr, Sunlight-Induced Molecular Progression of Oil into Oxidized Oil Soluble Species, Interfacial Material, and Dissolved Organic Matter, *Energy Fuels*, 2020, **34**, 4721–4726.

24 B. De Witte, C. Walgraeve, K. Demeestere and H. Van Langenhove, Oxygenated polycyclic aromatic hydrocarbons in mussels: analytical method development and occurrence in the Belgian coastal zone, *Environ. Sci. Pollut. Res.*, 2019, **26**, 9065–9078.

25 H. P. H. Arp, S. Lundstedt, S. Josefsson, G. Cornelissen, A. Enell, A.-S. Allard and D. B. Kleja, Native Oxy-PAHs, N-PACs, and PAHs in Historically Contaminated Soils from Sweden, Belgium, and France: Their Soil-Porewater Partitioning Behavior, Bioaccumulation in Enchytraeus crypticus, and Bioavailability, *Environ. Sci. Technol.*, 2014, **48**, 11187–11195.

26 S. Josefsson, H. P. H. Arp, D. B. Kleja, A. Enell and S. Lundstedt, Determination of polyoxymethylene (POM) – water partition coefficients for oxy-PAHs and PAHs, *Chemosphere*, 2015, **119**, 1268–1274.

27 C. L. Lemieux, I. B. Lambert, S. Lundstedt, M. Tysklind and P. A. White, Mutagenic hazards of complex polycyclic aromatic hydrocarbon mixtures in contaminated soil, *Environ. Toxicol. Chem.*, 2008, **27**, 978–990.

28 S. Lundstedt, P. A. White, C. L. Lemieux, K. D. Lynes, I. B. Lambert, L. Öberg, P. Haglund and M. Tysklind, Sources, Fate, and Toxic Hazards of Oxygenated Polycyclic Aromatic Hydrocarbons (PAHs) at PAH- contaminated Sites, *Ambio*, 2007, **36**, 475–485.

29 E. Wincent, M. E. Jönsson, M. Bottai, S. Lundstedt and K. Dreij, Aryl Hydrocarbon Receptor Activation and Developmental Toxicity in Zebrafish in Response to Soil Extracts Containing Unsubstituted and Oxygenated PAHs, *Environ. Sci. Technol.*, 2015, **49**, 3869–3877.

30 R. A. Frank, R. Kavanagh, B. Kent Burnison, G. Arsenault, J. V. Headley, K. M. Peru, G. Van Der Kraak and K. R. Solomon, Toxicity assessment of collected fractions from an extracted naphthenic acid mixture, *Chemosphere*, 2008, **72**, 1309–1314.

31 J. M. Gutierrez-Villagomez, K. M. Peru, C. Edington, J. V. Headley, B. D. Pauli and V. L. Trudeau, Naphthenic Acid Mixtures and Acid-Extractable Organics from Oil Sands Process-Affected Water Impair Embryonic Development of Silurana (Xenopus) tropicalis, *Environ. Sci. Technol.*, 2019, **53**, 2095–2104.

32 J. R. Marentette, R. A. Frank, A. J. Bartlett, P. L. Gillis, L. M. Hewitt, K. M. Peru, J. V. Headley, P. Brunswick, D. Shang and J. L. Parrott, Toxicity of naphthenic acid fraction components extracted from fresh and aged oil sands process-affected waters, and commercial naphthenic acid mixtures, to fathead minnow (Pimephales promelas) embryos, *Aquat. Toxicol.*, 2015, **164**, 108–117.

33 S. D. Melvin, C. M. Lanctôt, P. M. Craig, T. W. Moon, K. M. Peru, J. V. Headley and V. L. Trudeau, Effects of naphthenic acid exposure on development and liver metabolic processes in anuran tadpoles, *Environ. Pollut.*, 2013, **177**, 22–27.

34 J. V. Headley, K. M. Peru and M. P. Barrow, Mass spectrometric characterization of naphthenic acids in environmental samples: A review, *Mass Spectrom. Rev.*, 2009, **28**, 121–134.

35 M. P. Barrow, J. V. Headley, K. M. Peru and P. J. Derrick, Fourier transform ion cyclotron resonance mass spectrometry of principal components in oilsands naphthenic acids, *J. Chromatogr. A*, 2004, **1058**, 51–59.

36 X. Ortiz, K. J. Jobst, E. J. Reiner, S. M. Backus, K. M. Peru, D. W. McMartin, G. O'Sullivan, V. Y. Taguchi and J. V. Headley, Characterization of Naphthenic Acids by Gas Chromatography-Fourier Transform Ion Cyclotron Resonance Mass Spectrometry, *Anal. Chem.*, 2014, **86**, 7666–7673.

37 K. M. Peru, M. J. Thomas, D. C. Palacio Lozano, D. W. McMartin, J. V. Headley and M. P. Barrow, Characterization of oil sands naphthenic acids by negative-ion electrospray ionization mass spectrometry: Influence of acidic *versus* basic transfer solvent, *Chemosphere*, 2019, **222**, 1017–1024.

38 R. Hindle, M. Noestheden, K. Peru and J. Headley, Quantitative analysis of naphthenic acids in water by liquid chromatography–accurate mass time-of-flight mass spectrometry, *J. Chromatogr. A*, 2013, **1286**, 166–174.

39 E. A. Whisenhant, P. Zito, D. C. Podgorski, A. M. McKenna, Z. C. Redman and P. L. Tomco, Unique Molecular Features of Water-Soluble Photo-Oxidation Products among Refined Fuels, Crude Oil, and Herded Burnt Residue under High Latitude Conditions, *ACS ES&T Water*, 2022, **2**, 994–1002.

40 D. Dissing and G. Wendler, Solar Radiation Climatology of Alaska, *Theor. Appl. Climatol.*, 1998, **61**, 161–175.

© 2023 The Author(s). Published by the Royal Society of Chemistry

Environ. Sci.: Adv., 2023, **2**, 447–461 | **457**

41 M. Atkinson and C. Bingman, Elemental composition of commercial seasalts, *J. Aquaric. Aquat. Sci.*, 1997, **8**, 39–43.

42 A. Stubbins and T. Dittmar, Low volume quantification of dissolved organic carbon and dissolved nitrogen, *Limnol. Oceanogr.: Methods*, 2012, **10**, 347–352.

43 R. G. M. Spencer, L. Bolton and A. Baker, Freeze/thaw and pH effects on freshwater dissolved organic matter fluorescence and absorbance properties from a number of UK locations, *Water Res.*, 2007, **41**, 2941–2950.

44 M. M. Tfaily, D. C. Podgorski, J. E. Corbett, J. P. Chanton and W. T. Cooper, Influence of acidification on the optical properties and molecular composition of dissolved organic matter, *Anal. Chim. Acta*, 2011, **706**, 261–267.

45 M. Yan, Q. Fu, D. Li, G. Gao and D. Wang, Study of the pH influence on the optical properties of dissolved organic matter using fluorescence excitation–emission matrix and parallel factor analysis, *J. Lumin.*, 2013, **142**, 103–109.

46 P. Kowalczuk, W. J. Cooper, R. F. Whitehead, M. J. Durako and W. Sheldon, Characterization of CDOM in an organic-rich river and surrounding coastal ocean in the South Atlantic Bight, *Aquat. Sci.*, 2003, **65**, 384–401.

47 T. Ohno, Fluorescence Inner-Filtering Correction for Determining the Humification Index of Dissolved Organic Matter, *Environ. Sci. Technol.*, 2002, **36**, 742–746.

48 K. R. Murphy, C. A. Stedmon, D. Graeber and R. Bro, Fluorescence spectroscopy and multi-way techniques. PARAFAC, *Anal. Methods*, 2013, **5**, 6557–6566.

49 R. A. Harshman and M. E. Lundy, PARAFAC: Parallel factor analysis, *Comput. Stat. Data Anal.*, 1994, **18**, 39–72.

50 C. A. Stedmon and R. Bro, Characterizing dissolved organic matter fluorescence with parallel factor analysis: a tutorial, *Limnol. Oceanogr.: Methods*, 2008, **6**, 572–579.

51 K. R. Murphy, C. A. Stedmon, P. Wenig and R. Bro, OpenFluor– an online spectral library of auto-fluorescence by organic compounds in the environment, *Anal. Methods*, 2014, **6**, 658–661.

52 T. Dittmar, B. Koch, N. Hertkorn and G. Kattner, A simple and efficient method for the solid-phase extraction of dissolved organic matter (SPE-DOM) from seawater, *Limnol. Oceanogr.: Methods*, 2008, **6**, 230–235.

53 P. Zito, R. Ghannam, B. A. Bekins and D. C. Podgorski, Examining the Extraction Efficiency of Petroleum-Derived Dissolved Organic Matter in Contaminated Groundwater Plumes, *Groundwater Monit. Rem.*, 2019, **39**, 25–31.

54 J. A. Hawkes, J. D'Andrilli, J. N. Agar, M. P. Barrow, S. M. Berg, N. Catalán, H. Chen, R. K. Chu, R. B. Cole, T. Dittmar, R. Gavard, G. Gleixner, P. G. Hatcher, C. He, N. J. Hess, R. H. S. Hutchins, A. Ijaz, H. E. Jones, W. Kew, M. Khaksari, D. C. Palacio Lozano, J. Lv, L. R. Mazzoleni, B. E. Noriega-Ortega, H. Osterholz, N. Radoman, C. K. Remucal, N. D. Schmitt, S. K. Schum, Q. Shi, C. Simon, G. Singer, R. L. Sleighter, A. Stubbins, M. J. Thomas, N. Tolic, S. Zhang, P. Zito and D. C. Podgorski, An international laboratory comparison of dissolved organic matter composition by high resolution mass spectrometry: Are we getting the same answer?, *Limnol. Oceanogr.: Methods*, 2020, **18**, 235–258.

55 T. P. Fan, Characterization of naphthenic acids in petroleum by fast atom bombardment mass spectrometry, *Energy Fuels*, 1991, **5**, 371–375.

56 F. M. Holowenko, M. D. MacKinnon and P. M. Fedorak, Characterization of naphthenic acids in oil sands wastewaters by gas chromatography-mass spectrometry, *Water Res.*, 2002, **36**, 2843–2855.

57 B. P. Koch and T. Dittmar, From mass to structure: an aromaticity index for high-resolution mass data of natural organic matter, *Rapid Commun. Mass Spectrom.*, 2006, **20**, 926–932.

58 J. A. O'Donnell, G. R. Aiken, K. D. Butler, F. Guillemette, D. C. Podgorski and R. G. M. Spencer, DOM composition and transformation in boreal forest soils: The effects of temperature and organic-horizon decomposition state, *J. Geophys. Res.: Biogeosci.*, 2016, **121**, 2727–2744.

59 T. Šantl-Temkiv, K. Finster, T. Dittmar, B. M. Hansen, R. Thyrhaug, N. W. Nielsen and U. G. Karlson, Hailstones: A Window into the Microbial and Chemical Inventory of a Storm Cloud, *PLoS One*, 2013, **8**, e53550.

60 M. Guiñez, C. Bazan, L. D. Martinez and S. Cerutti, Determination of nitrated and oxygenated polycyclic aromatic hydrocarbons in water samples by a liquid–liquid phase microextraction procedure based on the solidification of a floating organic drop followed by solvent assisted back-extraction and liquid chromatography–tandem mass spectrometry, *Microchem. J.*, 2018, **139**, 164–173.

61 M. Eftekhardadkhah and G. Øye, Correlations between Crude Oil Composition and Produced Water Quality: A Multivariate Analysis Approach, *Ind. Eng. Chem. Res.*, 2013, **52**, 17315–17321.

62 A. Zsolnay, E. Baigar, M. Jimenez, B. Steinweg and F. Saccomandi, Differentiating with fluorescence spectroscopy the sources of dissolved organic matter in soils subjected to drying, *Chemosphere*, 1999, **38**, 45–50.

63 B. P. Hollebone, in *Handbook of Oil Spill Science and Technology*, 2014, pp. 37–50, DOI: 10.1002/9781118989982.ch2.

64 J. L. Weishaar, G. R. Aiken, B. A. Bergamaschi, M. S. Fram, R. Fujii and K. Mopper, Evaluation of Specific Ultraviolet Absorbance as an Indicator of the Chemical Composition and Reactivity of Dissolved Organic Carbon, *Environ. Sci. Technol.*, 2003, **37**, 4702–4708.

65 Z. Zhou, L. Guo, A. M. Shiller, S. E. Lohrenz, V. L. Asper and C. L. Osburn, Characterization of oil components from the Deepwater Horizon oil spill in the Gulf of Mexico using fluorescence EEM and PARAFAC techniques, *Mar. Chem.*, 2013, **148**, 10–21.

66 M. H. Mohamed, L. D. Wilson, J. V. Headley and K. M. Peru, Screening of oil sands naphthenic acids by UV-Vis absorption and fluorescence emission spectrophotometry, *J. Environ. Sci. Health, Part A: Toxic/Hazard. Subst. Environ. Eng.*, 2008, **43**, 1700–1705.

67 C. A. Stedmon and S. Markager, Tracing the production and degradation of autochthonous fractions of dissolved

organic matter by fluorescence analysis, *Limnol. Oceanogr.*, 2005, **50**, 1415–1426.

68 S. Retelletti Brogi, G. Cossarini, G. Bachi, C. Balestra, E. Camatti, R. Casotti, G. Checcucci, S. Colella, V. Evangelista, F. Falcini, F. Francocci, T. Giorgino, F. Margiotta, M. Ribera d'Alcalà, M. Sprovieri, S. Vestri and C. Santinelli, Evidence of Covid-19 lockdown effects on riverine dissolved organic matter dynamics provides a proof-of-concept for needed regulations of anthropogenic emissions, *Sci. Total Environ.*, 2022, **812**, 152412.

69 K. R. Murphy, G. M. Ruiz, W. T. M. Dunsmuir and T. D. Waite, Optimized Parameters for Fluorescence-Based Verification of Ballast Water Exchange by Ships, *Environ. Sci. Technol.*, 2006, **40**, 2357–2362.

70 K. R. Murphy, A. Hambly, S. Singh, R. K. Henderson, A. Baker, R. Stuetz and S. J. Khan, Organic Matter Fluorescence in Municipal Water Recycling Schemes: Toward a Unified PARAFAC Model, *Environ. Sci. Technol.*, 2011, **45**, 2909–2916.

71 K. Lu, H. Gao, H. Yu, D. Liu, N. Zhu and K. Wan, Insight into variations of DOM fractions in different latitudinal rural black-odor waterbodies of eastern China using fluorescence spectroscopy coupled with structure equation model, *Sci. Total Environ.*, 2022, **816**, 151531.

72 M. H. Jeon, J. Jung, M. O. Park, S. Aoki, T.-W. Kim and S.-K. Kim, Tracing Circumpolar Deep Water and glacial meltwater using humic-like fluorescent dissolved organic matter in the Amundsen Sea, Antarctica, *Mar. Chem.*, 2021, **235**, 104008.

73 C. DeFrancesco and C. Guéguen, Long-term Trends in Dissolved Organic Matter Composition and Its Relation to Sea Ice in the Canada Basin, Arctic Ocean (2007–2017), *J. Geophys. Res.: Oceans*, 2021, **126**, e2020JC016578.

74 D. C. Podgorski, P. Zito, J. T. McGuire, D. Martinovic-Weigelt, I. M. Cozzarelli, B. A. Bekins and R. G. M. Spencer, Examining Natural Attenuation and Acute Toxicity of Petroleum-Derived Dissolved Organic Matter with Optical Spectroscopy, *Environ. Sci. Technol.*, 2018, **52**, 6157–6166.

75 D. C. Podgorski, P. Zito, A. M. Kellerman, B. A. Bekins, I. M. Cozzarelli, D. F. Smith, X. Cao, K. Schmidt-Rohr, S. Wagner, A. Stubbins and R. G. M. Spencer, Hydrocarbons to carboxyl-rich alicyclic molecules: A continuum model to describe biodegradation of petroleum-derived dissolved organic matter in contaminated groundwater plumes, *J. Hazard. Mater.*, 2021, **402**, 123998.

76 M. C. R. Remolina, Z. Li and N. M. Peleato, Application of machine learning methods for rapid fluorescence-based detection of naphthenic acids and phenol in natural surface waters, *J. Hazard. Mater.*, 2022, **430**, 128491.

77 F. Berthou, J. Ducreux and G. Bodennec, Analysis of Water-Soluble Acidic Compounds Derived from Spilled Oil in a Controlled Marine Enclosure, *Int. J. Environ. Anal. Chem.*, 1985, **21**, 267–282.

78 C. A. Stedmon, S. Markager, L. Tranvik, L. Kronberg, T. Slätis and W. Martinsen, Photochemical production of ammonium and transformation of dissolved organic matter in the Baltic Sea, *Mar. Chem.*, 2007, **104**, 227–240.

79 M. Søndergaard, C. A. Stedmon and N. H. Borch, Fate of terrigenous dissolved organic matter (DOM) in estuaries: Aggregation and bioavailability, *Ophelia*, 2003, **57**, 161–176.

80 M. A. Smith, J. S. Kominoski, E. E. Gaiser, R. M. Price and T. G. Troxler, Stormwater Runoff and Tidal Flooding Transform Dissolved Organic Matter Composition and Increase Bioavailability in Urban Coastal Ecosystems, *J. Geophys. Res.: Biogeosci.*, 2021, **126**, e2020JG006146.

81 A.-R. Schittich, U. J. Wünsch, H. V. Kulkarni, M. Battistel, H. Bregnhøj, C. A. Stedmon and U. S. McKnight, Investigating Fluorescent Organic-Matter Composition as a Key Predictor for Arsenic Mobility in Groundwater Aquifers, *Environ. Sci. Technol.*, 2018, **52**, 13027–13036.

82 D. Graeber, Y. Tenzin, M. Stutter, G. Weigelhofer, T. Shatwell, W. von Tümpling, J. Tittel, A. Wachholz, D. Borchardt and D. O. C. Bioavailable, reactive nutrient ratios control heterotrophic nutrient assimilation—An experimental proof of the macronutrient-access hypothesis, *Biogeochemistry*, 2021, **155**, 1–20.

83 M. Derrien, M.-S. Kim, G. Ock, S. Hong, J. Cho, K.-H. Shin and J. Hur, Estimation of different source contributions to sediment organic matter in an agricultural-forested watershed using end member mixing analyses based on stable isotope ratios and fluorescence spectroscopy, *Sci. Total Environ.*, 2018, **618**, 569–578.

84 T. B. Bittar, S. A. Berger, L. M. Birsa, T. L. Walters, M. E. Thompson, R. G. M. Spencer, E. L. Mann, A. Stubbins, M. E. Frischer and J. A. Brandes, Seasonal dynamics of dissolved, particulate and microbial components of a tidal saltmarsh-dominated estuary under contrasting levels of freshwater discharge, *Estuarine, Coastal Shelf Sci.*, 2016, **182**, 72–85.

85 K. H. Altgelt and M. M. Boduszynski, *Composition and Analysis of Heavy Petroleum Fractions*, 1st edn, 1994.

86 S. Kim, R. W. Kramer and P. G. Hatcher, Graphical Method for Analysis of Ultrahigh-Resolution Broadband Mass Spectra of Natural Organic Matter, the Van Krevelen Diagram, *Anal. Chem.*, 2003, **75**, 5336–5344.

87 A. V. Callaghan, Metabolomic investigations of anaerobic hydrocarbon-impacted environments, *Curr. Opin. Biotechnol.*, 2013, **24**, 506–515.

88 N. Das and P. Chandran, Microbial degradation of petroleum hydrocarbon contaminants: an overview, *Biotechnol. Res. Int*, 2011, **2011**, 941810.

89 G. Fuchs, M. Boll and J. Heider, Microbial degradation of aromatic compounds — from one strategy to four, *Nat. Rev. Microbiol.*, 2011, **9**, 803–816.

90 J. Heider, Adding handles to unhandy substrates: anaerobic hydrocarbon activation mechanisms, *Curr. Opin. Chem. Biol.*, 2007, **11**, 188–194.

91 L. K. Oberding and L. M. Gieg, Methanogenic Paraffin Biodegradation: Alkylsuccinate Synthase Gene

© 2023 The Author(s). Published by the Royal Society of Chemistry

Environ. Sci.: Adv., 2023, **2**, 447–461 | **459**

Quantification and Dicarboxylic Acid Production, *Appl. Environ. Microbiol.*, 2018, **84**, e01773-17.

92 C. R. A. Toth and L. M. Gieg, Time Course-Dependent Methanogenic Crude Oil Biodegradation: Dynamics of Fumarate Addition Metabolites, Biodegradative Genes, and Microbial Community Composition, *Front. Microbiol.*, 2018, **8**, 2610.

93 H. P. Bacosa, D. L. Erdner and Z. Liu, Differentiating the roles of photooxidation and biodegradation in the weathering of Light Louisiana Sweet crude oil in surface water from the Deepwater Horizon site, *Mar. Pollut. Bull.*, 2015, **95**, 265–272.

94 S. Bobinger and J. T. Andersson, Photooxidation Products of Polycyclic Aromatic Compounds Containing Sulfur, *Environ. Sci. Technol.*, 2009, **43**, 8119–8125.

95 P. Campo, A. D. Venosa and M. T. Suidan, Biodegradability of Corexit 9500 and Dispersed South Louisiana Crude Oil at 5 and 25 °C, *Environ. Sci. Technol.*, 2013, **47**, 1960–1967.

96 T. K. Dutta and S. Harayama, Fate of Crude Oil by the Combination of Photooxidation and Biodegradation, *Environ. Sci. Technol.*, 2000, **34**, 1500–1505.

97 R. M. Garrett, I. J. Pickering, C. E. Haith and R. C. Prince, Photooxidation of Crude Oils, *Environ. Sci. Technol.*, 1998, **32**, 3719–3723.

98 S. M. King, P. A. Leaf, A. C. Olson, P. Zito and M. A. Tarr, Photolytic and photocatalytic degradation of surface oil from the Deepwater Horizon spill, *Chemosphere*, 2014, **95**, 415–422.

99 R. C. Prince, R. M. Garrett, R. E. Bare, M. J. Grossman, T. Townsend, J. M. Suflita, K. Lee, E. H. Owens, G. A. Sergy, J. F. Braddock, J. E. Lindstrom and R. R. Lessard, The Roles of Photooxidation and Biodegradation in Long-term Weathering of Crude and Heavy Fuel Oils, *Spill Sci. Technol. Bull.*, 2003, **8**, 145–156.

100 M. Seidel, S. Kleindienst, T. Dittmar, S. B. Joye and P. M. Medeiros, Biodegradation of crude oil and dispersants in deep seawater from the Gulf of Mexico: Insights from ultra-high resolution mass spectrometry, *Deep Sea Res., Part II*, 2016, **129**, 108–118.

101 Z. Yang, G. Zhang, B. P. Hollebone, C. E. Brown, C. Yang, P. Lambert, Z. Wang, M. Landriault and K. Shah, Fate of oxygenated intermediates in solar irradiated diluted bitumen mixed with saltwater, *Environ. Pollut.*, 2017, **231**, 622–634.

102 Z. Yang, C. Yang, G. Zhang, K. Shah, B. Chen, B. P. Hollebone, P. Jackman and V. Beaulac, Effects of asphaltenes on the photolytic and toxic behavior of bitumen and conventional oil products on saltwater, *J. Hazard. Mater.*, 2022, **436**, 129137.

103 N. M. F. M. Sampaio, J. Crucello, I. M. Junior, R. M. Carvalho and L. W. Hantao, Automated filtering scripts based on accurate mass applied to comprehensive two-dimensional gas chromatography coupled to high resolution mass spectrometry for group-type analysis of naphthenic acids, *J. Chromatogr. Open*, 2022, **2**, 100067.

104 P. Dong, Z. Chen, X. Qin and Y. Gong, Water Significantly Changes the Ring-Cleavage Process During Aqueous

105 R. A. Frank, K. Fischer, R. Kavanagh, B. K. Burnison, G. Arsenault, J. V. Headley, K. M. Peru, G. V. D. Kraak and K. R. Solomon, Effect of Carboxylic Acid Content on the Acute Toxicity of Oil Sands Naphthenic Acids, *Environ. Sci. Technol.*, 2009, **43**, 266–271.

106 R. J. Kavanagh, R. A. Frank, B. K. Burnison, R. F. Young, P. M. Fedorak, K. R. Solomon and G. Van Der Kraak, Fathead minnow (Pimephales promelas) reproduction is impaired when exposed to a naphthenic acid extract, *Aquat. Toxicol.*, 2012, **116–117**, 34–42.

107 A. G. Scarlett, C. E. West, D. Jones, T. S. Galloway and S. J. Rowland, Predicted toxicity of naphthenic acids present in oil sands process-affected waters to a range of environmental and human endpoints, *Sci. Total Environ.*, 2012, **425**, 119–127.

108 J. Wang, X. Cao, Y. Huang and X. Tang, Developmental toxicity and endocrine disruption of naphthenic acids on the early life stage of zebrafish (Danio rerio), *J. Appl. Toxicol.*, 2015, **35**, 1493–1501.

109 J. R. Marentette, K. Sarty, A. M. Cowie, R. A. Frank, L. M. Hewitt, J. L. Parrott and C. J. Martyniuk, Molecular responses of Walleye (Sander vitreus) embryos to naphthenic acid fraction components extracted from fresh oil sands process-affected water, *Aquat. Toxicol.*, 2017, **182**, 11–19.

110 G. D. Morandi, S. B. Wiseman, M. Guan, X. W. Zhang, J. W. Martin and J. P. Giesy, Elucidating mechanisms of toxic action of dissolved organic chemicals in oil sands process-affected water (OSPW), *Chemosphere*, 2017, **186**, 893–900.

111 V. Nero, A. Farwell, L. E. J. Lee, T. Van Meer, M. D. MacKinnon and D. G. Dixon, The effects of salinity on naphthenic acid toxicity to yellow perch: Gill and liver histopathology, *Ecotoxicol. Environ. Saf.*, 2006, **65**, 252–264.

112 K. D. Duncan, J. A. Hawkes, M. Berg, B. Clarijs, C. G. Gill, J. Bergquist, I. Lanekoff and E. T. Krogh, Membrane Sampling Separates Naphthenic Acids from Biogenic Dissolved Organic Matter for Direct Analysis by Mass Spectrometry, *Environ. Sci. Technol.*, 2022, **56**, 3096–3105.

113 J. M. Gutierrez-Villagomez, C. J. Martyniuk, L. Xing, V. S. Langlois, B. D. Pauli, J. M. Blais and V. L. Trudeau, Transcriptome Analysis Reveals That Naphthenic Acids Perturb Gene Networks Related to Metabolic Processes, Membrane Integrity, and Gut Function in Silurana (Xenopus) tropicalis Embryos, *Front. Mar. Sci.*, 2019, **6**, 533.

114 J. V. Headley, K. M. Peru and M. P. Barrow, Advances in mass spectrometric characterization of naphthenic acids fraction compounds in oil sands environmental samples and crude oil—A review, *Mass Spectrom. Rev.*, 2016, **35**, 311–328.

115 R. F. Lee, Photo-oxidation and Photo-toxicity of Crude and Refined Oils, *Spill Sci. Technol. Bull.*, 2003, **8**, 157–162.

116 S. M. Pomfret, R. B. Brua, D. Milani and A. G. Yates, Metabolomic Analysis of Hexagenid Mayflies Exposed to

Photooxidation of Toluene, *Environ. Sci. Technol.*, 2021, **55**, 16316–16325.

Sublethal Concentrations of Naphthenic Acid, *Front. Mol. Biosci.*, 2021, **8**, 669082.

117 D. Schemeth, N. J. Nielsen and J. H. Christensen, SPE-LC-MS investigations for the isolation and fractionation of acidic oil degradation products, *Anal. Chim. Acta*, 2018, **1038**, 182–190.

118 L. St. Mary, L. S. D. Trine, C. Roper, J. Wiley, S. L. Massey Simonich, M. McCoustra and T. B. Henry, Time-Related Alteration of Aqueous-Phase Anthracene and Phenanthrene Photoproducts in the Presence of TiO2 Nanoparticles, *Environ. Sci. Technol.*, 2021, **55**, 3727–3735.

119 H. Yu, Environmental Carcinogenic Polycyclic Aromatic Hydrocarbons: Photochemistry and Phototoxicity, *J. Environ. Sci. Health, Part C: Environ. Carcinog. Ecotoxicol. Rev.*, 2002, **20**, 149–183.

120 B. A. Bekins, J. C. Brennan, D. E. Tillitt, I. M. Cozzarelli, J. M. Illig and D. Martinović-Weigelt, Biological Effects of Hydrocarbon Degradation Intermediates: Is the Total Petroleum Hydrocarbon Analytical Method Adequate for Risk Assessment?, *Environ. Sci. Technol.*, 2020, **54**, 11396–11404.

© 2023 The Author(s). Published by the Royal Society of Chemistry

Environ. Sci.: Adv., 2023, **2**, 447–461 | **461**